INŽENÝRSKÁ MECHANIKA 2005
NÁRODNÍ KONFERENCE
s mezinárodní účastí
Svratka, Česká republika, 9. - 12. května 2005

MICROMECHANICS-HYDRATION MODEL FOR THE ELASTIC PROPERTIES OF A CEMENT PASTE

V. Šmilauer[1], **Z. Bittnar**[2]

Summary: *Cement paste is the important component of other engineering heterogeneous materials, such as various kinds of concrete. Using the micromechanic approach, intrinsic elastic properties of individual components of cement paste are upscaled to the scale of tens of micrometers. Cement hydration model has been developed for a prediction of microstructures of hydrating cement paste and in combination with micromechanics provides sufficient tool for prediction of elastic properties. Both models are discussed as well as the computational requirements of homogenization. Validation on the pastes with water-to-cement ratii 0.2 - 0.5 shows good correlation with experiments.*

1. Introduction

Modulus of elasticity (E) and Poisson ratio (ν) are important parameters in cement-based materials within structural design and analysis. Physical and chemical change in the microstructure of cement paste leads to the evolution of elastic properties. In contrast with strength, which is related mainly to porosity, elastic behavior reflects intrinsic mechanical values of individual components and their connectedness. The overall macroscopic response of microstructure lies always in the range of intrinsic values of components and determines usage of cement-based material. Rapidly developing techniques of homogenization allow analytical and numerical determination of elastic effective properties on the random hydrating cement microstructure.

The aim of this paper is to relate effective properties of cement paste to the properties of its individual chemical phases on nano and micro level. Such approach enables prediction at arbitrary time during hydration, considering all interacting phases. It is assumed that reactants and products keep specific elastic properties during the whole cement hydration procedure, only volume fraction changes as well as spatial configuration. Thanks to the development of nanoindentation technique and microscopy, elastic properties of isolated constituents may be accessed at very fine scales. While macroscopic elastic behavior of the cement paste has been studied and measured for decades, the role of microstructure remained unexplored for long times.

[1]Ing. Vít Šmilauer, Czech Technical University in Prague, Faculty of Civil Engineering, Department of Structural Mechanics, Thákurova 7, Praha 6, 166 29, vit.smilauer@fsv.cvut.cz

[2]Prof. Ing. Zdeněk Bittnar, DrSc., Czech Technical University in Prague, Faculty of Civil Engineering, Department of Structural Mechanics, Thákurova 7, Praha 6, 166 29, bittnar@fsv.cvut.cz

2. Model of cement hydration

Cement hydration model CEMHYD3D, developed ad NIST, is based on observing the development of 2D microstructure under the electron microscope [1]. The idea is to split up a microstructure into voxels (volume elements), typically with an edge of 1 μm. A voxel should be considered as an collection of a phase from the neighborhood, maintaining stoichiometry of chemical reactions and slightly deforming the real shape of microstructure. The size of voxel determines the model resolution that should be small enough to capture the important undergoing processes, e.g. dissolution, transport and diffusion. This coincides with the resolution of experimental devices where accurate identification of chemical phases is expected to be as fine as possible.

The chemical formulas are written in the nomenclature of the cement chemistry, e.g. C=CaO, S=SiO_2, A=Al_2O_3, H=H_2O. Model of cement hydration is built up on the four important phases of cement paste that significantly determine resulting behavior.

- unhydrated cement clinker: C_3S, C_2S, C_3A, C_4AF
- calcium hydroxide: CH
- C-S-H phases
- water-filled and empty porosity

The 3D microstructure consists of chemical phases distributed within a representative cube which is implemented as ID assignment to each voxel. The rules how to handle individual voxels are called cellular automata and they define how voxels dissolve, move and what happens on their collision. Cellular automata are combined with probabilistic functions that were found effective in the description within considered model [3]. Hydration products are, with certain probabilities, formed on the grains exposed to water contact and they nucleate in the available pore space.

The reconstruction of initial 3D microstructure with a 1 μm resolution uses autocorrelation function obtained from real cement powders [1]. Comprehensive database of cements may be found at the NIST virtual cement laboratory. The size of microstructure may be arbitrary, limiting the maximal cement grain that may be placed in. The microstructure remains periodic during all calculation which significantly simplifies following homogenization. A flowchart of the model with associated homogenization is in figure 1. Model cycles can be mapped on time axis using parabolic relationship [1]. Since this brings fitting parameter to the whole procedure, all results are further related to the degree of hydration, which define the ratio of hydrated to initial amount of cement.

Any model of a random system brings two sources of error: statistical fluctuation and finite size effect [3]. Statistical error emerge in any random system due to its representation, e.g. small dimensions of a cement paste. Finite size of representative cube captures only limited piece of material which means that the sample is not statistically homogeneous. The method how to eliminate these errors is in the size of the PUC (periodic unit cell). This model of cement hydration brings also digital resolution problems and the voxel size of 1 μm seems reasonable across various model application, e.g. percolation, simulated heat release, diffusivity or permeability [3].

Percolation theory describes topological connection in a random material of at least two

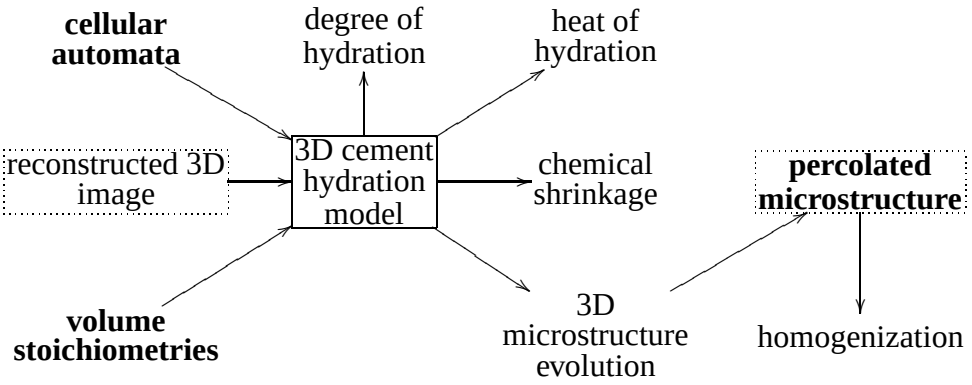

Figure 1: A flowchart of CEMHYD3D model and homogenization process, adapted from [1].

phases. Cement paste starts as a liquid mixture of cement, water and additives. As the time elapses, the suspension is transformed to a solid, load bearing structure. The beginning of stiffening, or a set point, corresponds to a percolation threshold. Special algorithm is applied for accessing the connectivity of output digital images of the model [1]. Only mutually connected phases are taken into account in homogenization further. Physically this correspond to the connectivity of opposite sides of the PUC.

3. Numerical homogenization

The purpose of homogenization is to find a homogeneous medium that would behave in the same manner as the piece of a heterogeneous one. The shape of microstructure is a prerequisite for homogenization using numerical methods and, in contrast to the analytical analysis, brings new information introduced explicitly. There are several methods how to calculate effective properties numerically, e.g. static condensation, generalized method of cells, finite difference method, FEM or methods based on the fast Fourier transformation (FFT).

The digital image processing that leads to the digital microstructure reconstruction creates, in our case, periodic microstructure as the collection of voxels [4]. Following prerequisites were considered: regular elements in the PUC that may remain unconnected in a node due to the percolation phenomenon, relatively small size of the RVE (representative volume element), robust algorithm and convergence for high contrast values. The FEM is employed in all cases further since it holds for all above mentioned items.

Consider a volume element V, where conditions are prescribed on boundary ∂V in order to estimate effective properties:

- periodic boundary conditions are easy-to-apply since the output from the hydration model is periodic. The displacement field over the volume surface ∂V takes the form:

$$\boldsymbol{u}(\boldsymbol{x}) = \boldsymbol{v}(\boldsymbol{x}) \quad \forall \boldsymbol{x} \in V \tag{1}$$

  where $\boldsymbol{x}$ denotes the point of interest, $\boldsymbol{u}$ is the displacement field and $\boldsymbol{v}$ is the periodic field, where opposite nodes share the same displacement,

- kinematic uniform boundary conditions (KUBC), where the displacement on boundary ∂V is prescribed, based on homogeneous strain $\boldsymbol{E}$:

$$\boldsymbol{u}(\boldsymbol{x}) = \boldsymbol{E} \cdot \boldsymbol{x} \quad \forall \boldsymbol{x} \in \partial V \tag{2}$$

- static uniform boundary conditions (SUBC), where the traction is prescribed on boundary. Implementation to the FEM needs to transform the traction vector to the nodal force:

$$\boldsymbol{f}(\boldsymbol{x}) = A_i \boldsymbol{\Sigma} \cdot \boldsymbol{x} \quad \forall \boldsymbol{x} \in \partial V \tag{3}$$

  where $\boldsymbol{f}$ is the nodal force vector applied at the boundary nodes, A_i is the corresponding surface area around the node of applied traction, $\boldsymbol{\Sigma}$ is prescribed homogeneous stress.

For all situations of boundary conditions, the overall elastic moduli are calculated from average values from the whole body V:

$$\langle \boldsymbol{C} \rangle = \langle \boldsymbol{\sigma} \rangle : \langle \boldsymbol{\epsilon} \rangle \tag{4}$$

where the brackets $\langle\rangle$ represent the volume average of the given quantity. The ranges from the above mentioned three boundary conditions hold in inequality, in the sense of quadratic forms [6]:

$$\boldsymbol{C}^{SUBC} \leq \boldsymbol{C}^{PERIODIC} \leq \boldsymbol{C}^{KUBC} \tag{5}$$

Equation 5 expresses the influence of the boundary conditions on the homogenized volume. If the PUC is large enough, the effect of boundary conditions disappears and the results are the same for all three boundary conditions. These moduli will be recalled as apparent.

4. Mesh generation

The percolated output cement image serve as the input image of microstructure. To cover the period of cement hydration, typically 40 images of various age are analyzed for each cement paste. The hexahedral element in the cubic form has been found to describe well the performance of the microstructure. Example of the regular mesh, where periodic boundary conditions are applied, is in figure 2, the analyzed microstructure with phase assignment in figure 3. Note that the nodes with number 1 experience the same displacement in this particular case in all such points. This is implemented into the FEM code as the same code numbers.

Perfectly connected microstructure has uniform mesh where one vertex is common for all adjacent elements. In practical simulation, isolated clusters emerge, as in figure 4. These clusters are result of percolation and they remain physically unconnected to any cluster touching a cube side. Preliminary simulation of the cement paste revealed, that the microstructure is much stiffer than measured from experiments, especially at the beginning, when uniform mesh is used. While percolation takes into account a connection by side, FEM works on displacement at nodes. Certain nodes, that touch in some vertex within the spanning cluster, remain physically unconnected. This is denoted as multiple node in figure 4. Typical example are two different, adjacent cement grains which are embedded in one cluster and not connected directly. Uncoupling displacement in multiple nodes for appropriate elements may be a remedy of high stiffness and partially would corresponds to the mesh refinement around that point.

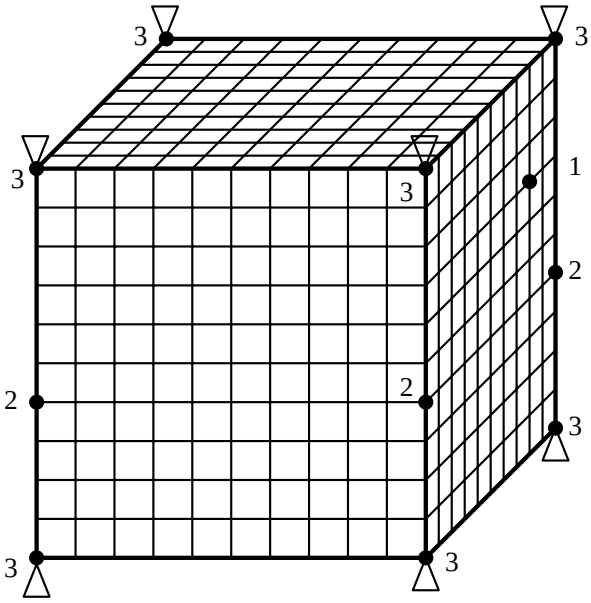

Figure 2: Periodic boundary conditions on the PUC.

Figure 3: Example of digital image at the degree of hydration of 0.3.

Numerical implementation of multiple node is clear from figure 5. Each central node has around 8 adjacent voxels, residing in the neighborhood of a central node. All appropriate nodes are attached to that central node and the disconnected nodes are left and assigned a different DOF's.

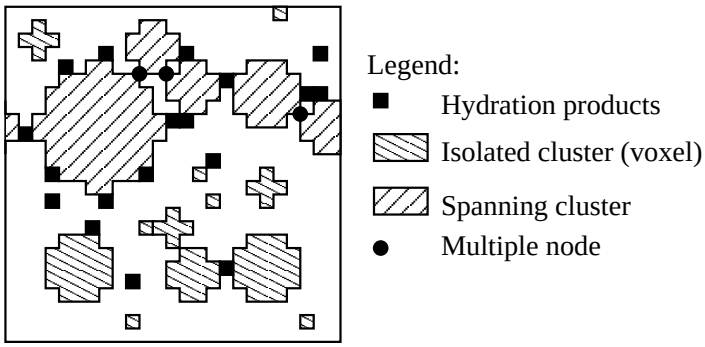

Figure 4: Example of 2D percolation in the cement microstructure.

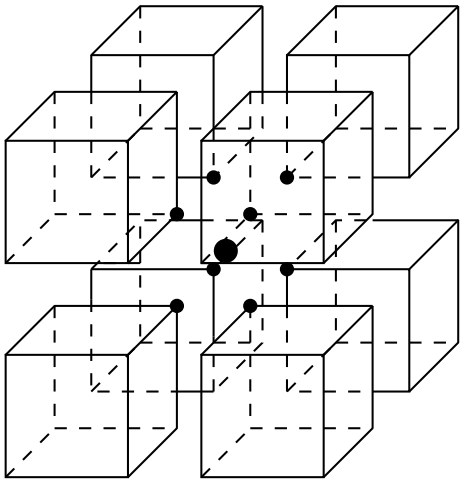

Figure 5: Multiple node configuration.

5. Intrinsic elastic properties

With the development of nanoindentation, elastic properties of constituents can be accessed at very fine scales. Typical indentation depth lies in the range of 300 to 500 nm. Results from nanoindentation together with the results from resonance frequency method are summarized in

table 1 for some clinker minerals. Higher scatter of values from nanoindentation reflects also higher intrinsic porosity.

Nanoindentation tests of C-S-H and calcium hydroxide were performed by Constantinides and Ulm, in an OPC with the *wcr* =0.5 [2]. They found two peaks in Young's modulus, that may be attributed to the two type: low and high density one (LD and HD), table 1. The prediction of these two types is extension of the model of cement hydration and may be found in [8].

Since calcium hydroxide and the two C-S-H types are the most common hydration products, effective properties of the cement paste rely considerably upon their elastic behavior. Other values from different sources used during homogenization are given in table 1.

phase	E (nanoind.) (mechanical)	ν	E (resonance)	porosity [%]	ref.
C_3S	**135**$\pm$7	**0.3**	147$\pm$5	2.38	[9]
C_2S	**130**$\pm$20	**0.3**	140$\pm$10	1.61	[9]
C_3A	**145**$\pm$10	**0.3**	160$\pm$10	3.63	[9]
C_4AF	**125**$\pm$20	**0.3**	-	-	[9]
$C\overline{S}H_2$	16-**30**-35	0.18-**0.3**-0.34	-	3.5-7.5	*
Porosity	$\mathbf{10^{-3}}$	**0.499**	-	-	-
CH	**38**$\pm$5	**0.305**	-	-	[2]
C-S-H_{LD}	**21.7**$\pm$2.2	**0.24**	-	-	[2]
C-S-H_{HD}	**29.4**$\pm$2.4	**0.24**	-	-	[2]
$C_6A\overline{S}_3H_{32}$	**22.4**	**0.25**	-	-	[5]
$C_4A\overline{S}H_{12}$	**42.3**	**0.324**	-	-	[5]
C_3AH_6	**22.4**	**0.25**	-	-	*
FH_3	**22.4**	**0.25**	-	-	*

Table 1: intrinsic elastic moduli of chemical phases in the model as measured by nanoindentation, resonance frequency or mechanical test. E moduli with standard deviation or range are in GPa.* values are estimated, based on [5].

6. Validation

First example covers ordinary CEM I with *wcr* = 0.5. Evolution of E-modulus is recalculated as a function of the capillary porosity from experiment [5].

In order to explore an effect of the microstructure size during whole hydration period, three microstructures with the edge of 25, 50, 75 μm were generated using the same PSD curve and autocorellation functions. Voxel edge and the resolution is 1 μm and each representative cube contained possible largest cement grain, i.e. the diameter of the half edge size. The model run 1500 cycles at a constant temperature for each microstructure. Figure 6 demonstrates effect of percolation on Young's modulus from the FEM in the microstructure with the edge of 25 μm. Unpercolated regular microstructure, i.e. considering all phases, yield non-zero apparent values from the beginning. Overestimation of E-moduli is the result of high stiffness of the

microstructure of the paste where some voxels are physically disconnected but not considered so in the FEM. Results are improved, when only spanning clusters are taken into account.

The effect of the microstructure size is in figure 7, with the multiple nodes considered. While the 25 μm size is insufficiently small and leads to a lower stiffness due to the percolation and statistically heterogeneous material, the difference between 50 and 75 μm size is negligible and correspond to experimental values during the whole hydration time.

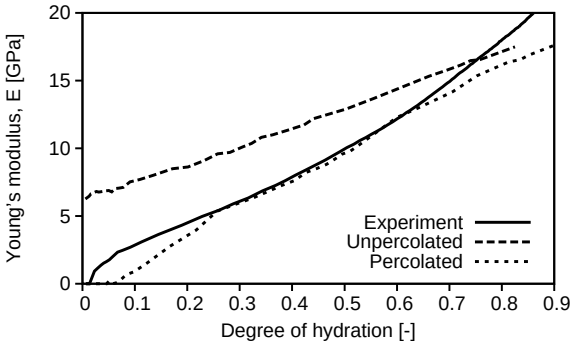

Figure 6: Effect of percolation on E-modulus, 25^3 μm, periodic [5].

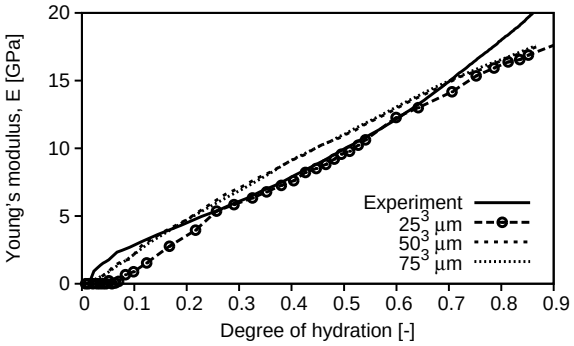

Figure 7: Effect of RVE size on E-modulus, periodic, multiple nodes.

Figures 8 and 9 show results from the FEM with the periodic boundary conditions, KUBC and SUBC at the degree of hydration (α) of 0.3 and 0.9. Results from regular and multiple-node microstructures are displayed as well, the bars in figures represent the 95 % confidence level. The precision of conjugate gradient method solver had to fit within 1 % of correct value, obtained by a significant number of iterations. Both figures imply that 1) the lower the degree of hydration, the larger size of RVE is necessary, 2) the multiple-node algorithm is unexchangeable for lower degree of hydration 3) the scatter decreases with larger RVE and more hydrated microstructure and 4) the bound of KUBC and SUBC are true according to equation 5.

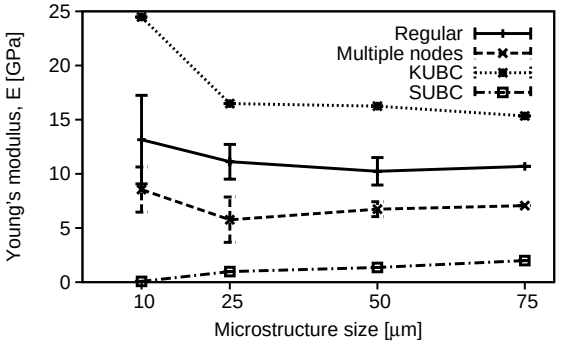

Figure 8: Effect of resolution on apparent E-modulus at α=0.3.

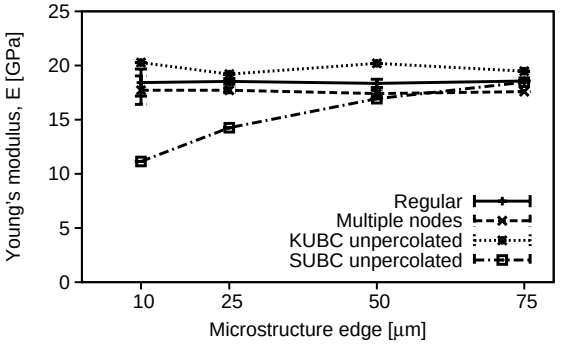

Figure 9: Effect of resolution on apparent E-modulus at α=0.9.

To study the effect of a dense microstructure, a cement paste with the *wcr* = 0.25 was used. Low *wcr* means that high portion of cement remains unhydrated during all hardening process, which means the maximum degree of hydration of about 0.65. The unhydrated clinker minerals boost the stiffness of the cement paste together with higher portion of C-S-H$_{HD}$.

An image of hydrated microstructure of the size 25^3 μm at the degree of hydration of 0.3 is in figure 3, the black color represents capillary porosity. The number of nodes for the multiple and regular mesh configuration with the edge of 75 μm is plotted in figure 11. The highest difference is found at the degree of hydration of 0.15 and, after all, converges to the regular mesh. Figure 11 shows results from different PUC sizes. Big discrepancy between experiment and FEM homogenization in the middle region points to the resolution problems and to the fitted relationship between Young's modulus and capillary porosity. The early and late values correspond well with data recalculated from experiment. The difference between 50 and 75 microstructure edge size is again not significant.

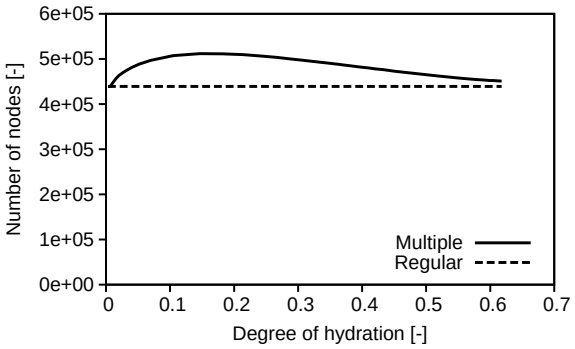

Figure 10: Number of nodes in two mesh configurations.

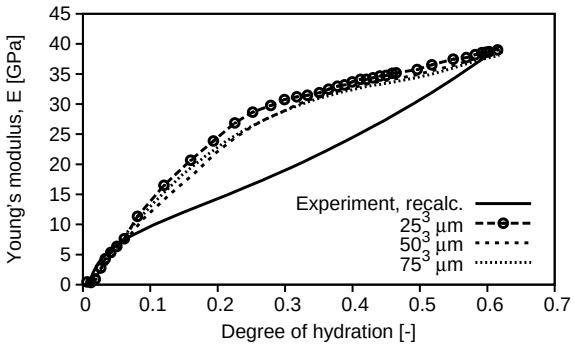

Figure 11: Effect of RVE size on E-modulus, periodic, multiple nodes.

The apparent moduli of different RVE sizes were explored again on edges of 10, 25, 50 and 75 μm, on five randomly generated samples for each size. The hydration model had the same configuration as in the paste with *wcr* = 0.5. Apparent moduli with 95 % confidence level for the FEM homogenization are in figures 12 and 13 for two hydration degrees. Young's moduli are much closer each other for regular and multiple-node configuration since the dense microstructure percolates sooner and connects well all phases in the PUC. No decrease of Young's modulus was found with the smaller size of 75^3 μm, and 0.6 % maximal difference is against the 50^3 μm size. This suggests that the 50 μm edge of the RVE is sufficient, at least for final hydration stages.

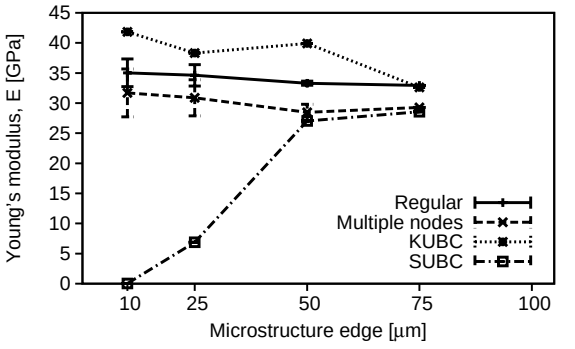

Figure 12: Boundary conditions, Young's modulus at α = 0.3 [5].

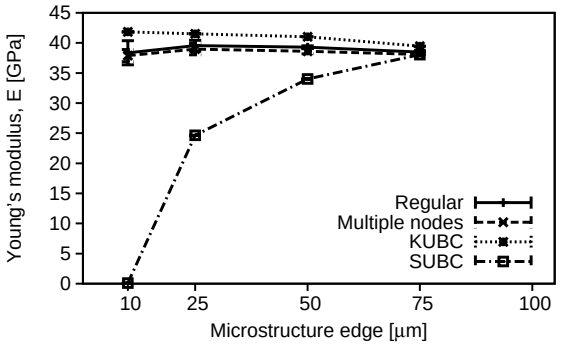

Figure 13: Boundary conditions, Young's modulus at α = 0.65.

7. Conclusion

This paper has presented combination of NIST cement hydration model and multiscale homogenization approach. Digital microstructures from the NIST model provided sufficient input data for elastic homogenization, taking into account percolation phenomena. It has been shown that percolation must be considered in the models at early ages of cement paste. Without accessing connectedness of chemical phases, physical micromechanic models remains unjustified. There are only few free parameters in the NIST model that influence effective properties, whole approach relies on intrinsic elastic mechanical properties and on commonly used cement chemistry reactions.

FEM numerical elastic homogenization, performed on digital images of NIST model, brings digital resolution problems. The reasonable microstructure size was found as 50x50x50 μm for a *wcr* in the range of 0.25-0.5. This roughly corresponds to the similar results obtained from variation of hydration degree [7]. Multiple node mesh yields always lower apparent E moduli then the regular mesh, substituting mesh refinement. Overestimation of E-modulus was observed at the dense microstructure with *wcr* = 0.25 and is probably attributed to the resolution of the NIST model and statistical inhomogeneity. Static and kinematic boundary conditions provided bounds of the RVE and for the periodic boundary conditions were found to have the smallest variation when the RVE size has changed.

8. Acknowledgement

Financial support of FRVŠ G1 2642 (Micromechanical analysis of cement paste structure) and GAČR GA103/03/1350 is gratefully acknowledged.

9. References

[1] Bentz, D.P. (2000) CEMHYD3D: A Three-Dimensional Cement Hydration and Microstructure Development Modeling Package. Version 2.0. *Manual*. Building and Fire Research Laboratory Gaithersburg, Maryland 20899.

[2] Constantinides G. & Ulm F.-J. (2004) The effect of two types of C-S-H on the elasticity of cement-based materials: results from nanoindentation and micromechanical modeling. *Cement and Concrete Research*, 34, pp. 67-80.

[3] Garboczi, E. J. & Bentz D. P. (2001) The effect of statistical fluctuation, finite size error, and digital resolution on the phase percolation and transport properties of the NIST cement hydration model. *Cement and Concrete Research*, 31, pp. 1501-1514.

[4] Garboczi E.J. & Day A.R (1995) An algorithm for computing the effective linear elastic properties of heterogeneous materials: three-dimensional results for composites with equal phase Poisson's ratios. *J. Mech. Phys. Solids*, 43, 9, pp. 1349-1362.

[5] Kamali S. , Moranville M. , Garboczi E., Prené S. & Gérard B. (2004) Hydrate dissolution influence on the Young's modulus of cement pastes. *Proc. 5th International Conference on Fracture Mechanics of Concrete and Concrete Structures, FraMCoS - 5, Colorado*.

[6] Kanit T. *et al.* (2003) Determination of the size of the representative volume element for random composites: statistical and numerical approach. *International Journal of Solids and Structures*, 40, pp. 3647-3679.

[7] Smilauer V. & Bittnar Z. (2004) Effects of representative cube size on the simulation of Portland cement hydration in CEMHYD3D model. *5th International PhD Symposium in Civil Engineering*, A. A. Balkema Publishers, pp. 581-587.

[8] Šmilauer V. & Bittnar Z. (2005) Mikromechanická předpověď elastických vlastností cementové pasty ze simulace hydratace. *Proc. Juniorstav 2005, Brno*, pp. 77-81.

[9] Velez K. *et al.* (2001) Determination by nanoindentation of elastic modulus and hardness of pure constituents of portland cement clinker. *Cement and Concrete Research*, 31, pp. 555-561.